Detection and Classification of Brain Tumours from MRI Images with Prediction of the Overall Survival Rate in Glioblastoma Using Machine Learning Techniques

Royyuru Srikanth[*1], Dr. N. Kanya[2], Dr. P. S. Rajakumar[3]

Abstract: Classifying a brain tumour is a crucial first step in establishing whether or not the abnormal tissues present a lethal threat to the patient and creating an appropriate treatment strategy for the latter's recovery. The most dangerous and rapidly-growing variety of glial tumour, glioblastoma multiforme (GBM) is most commonly referred to by its acronyms, glioblastoma. Most of the time, these tumours migrate to neighbouring brain tissue. Those with high grade glioma (GBM), which is highly aggressive and progresses quickly, have a poor survival rate compared to those with other tumours. Radiologist clinical decision-making and methodical treatment planning for patients can be enhanced by using survival time predictions (also known as OS time). Many imaging features of the brain, including the size and shape of the tumour, determine the outcome for the patient as a whole. In this paper, we used Random Forest, Support Vector Machines, XgBoost, and the Logistic Regression with Boosting Method (LGBM) to predict the overall survival (OS) period based on radiomic features. These radiomic characteristics are a combination of the tumor's deep characteristics and the characteristics that were shaped by hand. The prediction's reliability is dependent on the tumour volume being isolated from the various MRI modalities. Because of this, the U-Net++ deep model is used to recover the complete tumour and its subtumor from the multi-modal MR images, and then the pictures are stacked for deep feature extraction using convolutional neural networks. After feature reduction by principal component analysis (PCA) enhanced accuracy, the radiomic feature set was used for OS period forecasting. The accuracy of the forecast was examined utilising data from both two- and three-class survival analyses. An experiment was run using the popular BraTS 2017 dataset, and the findings indicated that several classifiers were able to reach an AUC value of 69% for a 3-class classification and a 67% AUC value for a 2-class group. The segmentation DOR is calculated to be 1269.29, which is greater than 2033.99 and lower than 648.00 for entire tumour, augmenting tumour, and necrotic tumour extraction, respectively. Both the genetic algorithm (GA) and the particle swarm optimisation (PSO) are used to the fused feature set to improve accuracy even further. Eventually, the approach achieves an area under the curve (AUC) score of 0.66 when employing fused features + SVM + GA (3-class group) and 0.70 when employing fused features + SVM + PSO, both of which are better than state-of-the-art methods (2-class group). Both of these results are higher than the minimum passing grade of 0.65.

Keywords: Survival prediction, Glioblastoma multiforme, Brain tumour segmentation, U-Net++, Machine learning

1. Introduction

Tumors, or neoplasms, develop when the uncontrolled division of aberrant cells goes on for too long [1]. The term "cancer" is commonly used to refer to a brain tumour, which is a mass of abnormal tissues located in either the central canal of the spinal column or the brain [2].Nevertheless, within this cluster, a few cells appear immune to the mechanisms normally responsible for controlling cell growth and division.Our rather inflexible skull encloses and shields our brain from any potential damage. The rapid growth of the tumour in such a small area hampers the brain's capacity to perform its typical activities. It's probable that major disorders, including prolonged exposure to inorganic compounds or genetic issues, are the key drivers of the development of deadly malignant cells in the brain.

Tumors in the brain can be either benign (not cancerous) or malignant (cancerous) (cancerous). The pressure inside the skull increases as benign tumours, precarcinomas, or malignant tumours grow, which can cause a number of serious health issues in people. This could cause irreversible brain damage and put the patient's life in danger. Medical photographs can be challenging to interpret and extract meaningful data from due to their subjective and complex nature.This is going to be a challenging endeavour. From the data collected, we may conclude that brain tumours account for between eighty-five and ninety percent of all primary CNS malignancies. Recently affected cases of brain and central nervous system (CNS) cancer were identified in [1]. These cancers account for about 3% of all other cancers. The number of

---
[1] *Research Scholar, Dept. of Computer Science & Engineering ,Dr.MGR Educational and Research Institute,Chennai , India*

[2] *Professor,Dept. of Information Technology ,Dr.MGR Educational and Research Institute,Chennai , India*

[3] *Professor,Dept. of Computer Science & Engineering, Dr.MGR Educational and Research Institute,Chennai , India*

* Corresponding Author Email: royyurusrikanth@gmail.com

reported cases is five times higher in European countries compared to those in Asia. Automated tumors segmentation is critical for early detection and successful treatment of brain tumours. The alternative, manual segmentation, is prohibitively time-consuming and costly. Automatic region of interest and vital information extraction has enhanced because to recent developments in image processing and computer vision. As a result, treatment planning is now easier to execute.

Brain damage can be caused by the growth of both malignant and noncancerous brain tumours. Tumors of the brain are solid neoplasms that form inside the brain's skull. These tumours form when brain tissue or cells grow abnormally and out of control. [3]. One of the most rapidly progressing primary tumours is a glioma, which develops from glial cells. Gliomas are classified as either low grade, which grow more slowly, or high grade, which are highly malignant tumours that put the patient's life in serious jeopardy. Glioblastoma multiforme, often known as GBM or glioblastoma, is the most malignant kind of glial tumour and develops rapidly. It is common for these tumours to spread to neighbouring brain areas. [4] The World Health Organization reports that the survival rate for people with HGG tumours is less than two years, but those with LGG can live for several years after diagnosis. [5] Most patients with these tumours will still die from their condition even with the most cutting-edge diagnostic tools, radiation therapy, and surgical procedures currently available. Survival rates for brain tumours have gained prominence in recent years, [6] giving radiologists a new point of reference for treatment strategy development. Because of the limited availability of labelled training subjects, the performance of PS prediction using existing approaches is decreasing.

In this research, we propose an approach to enhance glioma diagnosis accuracy. The most significant improvement brought about by the proposed plan is as follows:

1. The brain tumour is initially segmented using multimodal brain MR images and a U-Net++ model equipped with a weighted pooling mechanism. This must be completed before moving on to the next phase. Both the primary tumour and any augmenting subparts are included in this dissection.

2. The dataset includes 163 patients with at least one day of survival information, and a convolutional neural network is used to recover both manually-created and deep characteristics from all of the sub-tumor regions.

3. Determining the total amount of time spent alive is accomplished by a number of machine learning techniques, including the use of a combination of manually created features and deep features, to achieve higher precision. Finally, the bio-inspired optimisation

methodologies are put into practice to produce the required degree of performance.

Tumors are classified as either benign (non-cancerous) or malignant (cancerous) by the medical community based on their severity and degree of cancer. Figure 1 shows an example of this classification scheme. Initial brain tumours develop in an unaltered brain cell or in one of the tissues directly under its skull. This category of tumours accounts for the vast majority of malignant brain tumours. The majority of malignant brain tumours are gliomas. Depending on the circumstances, primary tumours may be harmless or malignant. In most cases, secondary tumours seen in the brain are malignant tumours that originated in another part of the body and metastasized there. [7] Almost a dozen types of brain tumours exist.
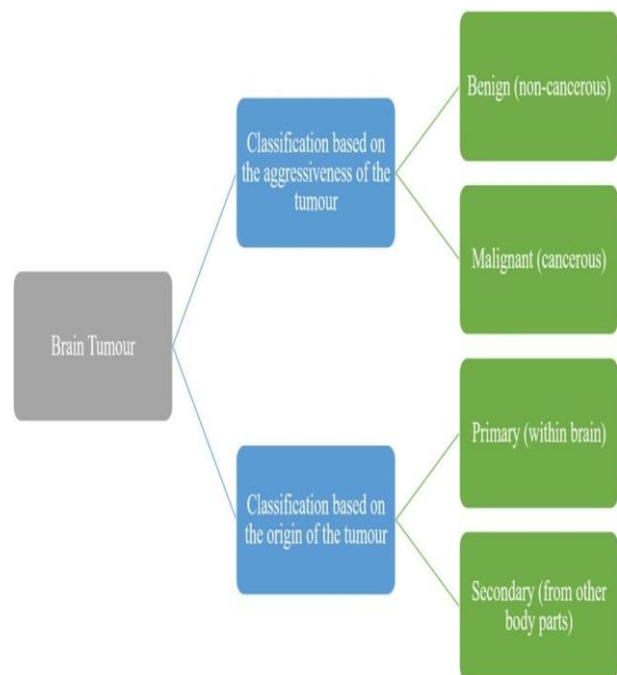

Fig 1. Brain tumours are classified into subgroups based on their aggressiveness and the site of initial diagnosis.

Some of the most lethal and aggressive tumours are malignant gliomas. The glial cells in the brain are the source of many diseases, and they can spread rapidly to other organs. The brain is rich in glial cells More than 60% of all malignant brain tumours found in adults are gliomas. Several forms of gliomas exist, with oligodendrogliomas, medulloblastomas, oligocytomas, and glioblastomas being the most common.

MRI scans have been shown to be effective in the context of clinical practise for documenting gliomas [8,9]. Medical image analysis often makes use of magnetic resonance imaging (MRI) because it does not require any sort of invasive procedure. The work was conducted out on the well-known8 dataset for the 2017 Multimodal Brain Tumor Segmentation Competition [10].This dataset includes MRI scans from 240 patients who were all

diagnosed with high-grade glioma. Typical structural MRI scans for humans measure 240 mm on the short axis (T1), 240 mm on the long axis (T2WI), and 155 mm in the transverse direction (T2FLAIR). The tumor's enhancing region (ET) is marked with the value 4, whereas the necrotic core region (NCR) is identified with the value 1, and the rest of the tumour is identified with the value 0. Machine learning techniques of various kinds were used to make predictions about the PS days based on these characteristics. Next to each patient's age in the dataset, the prognosis score (PS) is provided in days. Genetic algorithms and particle swarm optimisation (PSO) are used to improve prediction accuracy, and the survivors are divided into three groups based on their expected lifespan: a short group (<10 months), a medium group (>10 and <15 months), and a long group (>15 months) and 2-class: short (<12 months) and long (>12 months) group.

In this paper, the rest of the sections will be organized as follows: Section 2 Provides a summary of the several approaches of predicting future survival. In Section 3, detailed description of the proposed methodology implemented is presented. Section 4 describes experimental results analysis of the survival time. Finally, in Section 5 describes the conclusion and the future scope of the article are shown.

2. Related Work

Challenges remain in automatic brain tumour segmentation because of the wide variety of brain tumours that exist in terms of size, shape, location, and appearance. The fact that brain tumours come in so many different varieties presents unique difficulties. Both supervised and unsupervised methods can be used in the segmentation process. Several studies and methods, from the more traditional thresholding method to the more current deep learning approaches, have been created to segment brain tumours. Below, we highlight several research that are both very pertinent to the requested topic and just published. [11] In this study, we introduced a treatment planning tool that integrates multiple image processing techniques to improve brain image analysis results. Both of these fields could benefit from the use of this instrument. The accurate segmentation of vital organs from MRI and CT scans has previously been accomplished using a wide range of methods.

Segmentation is a technique used to extract useful information from images by first dividing them into smaller parts. In the realm of image processing, numerous segmentation methods exist, each of which may employ unique characteristics. Researchers typically utilise CNN, U-Net, and Segnet models, all of which are based on deep learning, to segment medical images because of their effectiveness and greater level of accuracy. The

performance of the network was measured across a number of benchmark datasets, and it was used in [12] to detect and segment brain tumours in MRI image patches. Using the HGG and LGG datasets published at the BraTS 2015 conference, we describe a fully automatic method for segmenting brain tumours based on U-Net and evaluate its performance. Prior to this work [13, 14], we used a cascading CNN deep learning model to segment brain tumours. Three learned convolutional layers, each tuned for a distinct part of the tumour, form the basis of this model. The results from BraTS 2015 and BraTS 2013 showed that a Dice score of 89% was adequate for full tumour segmentation. This segmentation method, which is based on RA-U-Net [15], first extracts the volume of interest (VOI) of a tumour and then segments the VOI into individual tumour cells. The approach's architecture is analogous to that of the 3D U-Net, which is based on the principle of encoding data in a way that accounts for its context. It is crucial in the U-Net design that the high-level and low-level feature maps be combined throughout the down sampling process. This improves the quality of the semantic segmentation. For more precise segmentation, it is recommended to employ a nested U-Net structure, which can be achieved by redesigning the skip connection [16].

In this paper, they address the challenges posed by U-Net means depth and its limited skip connection design. Some papers use transfer learning15 to determine whether a brain tumour is malignant or benign by segmenting it into individual cells. Two datasets, Ischemic Stroke Lesion Segmentation (ISLES) from 2018 and Multimodal Brain Tumor Segmentation (BRATS) from 2013-2016, are used for the evaluation of the method's efficacy.

Once the tumour has been segmented, the radiologist has a higher chance of saving the lives of patients with glioma by providing a precise prognosis of how long the patient will have to fight the cancer. Study 16 shows that textural elements extracted from MRI data may be useful for characterising genetic subgroups of GBM and predicting 12-month overall survival status for GBM patients without requiring procedures. The possibility of using this approach to characterise GBM has been considered. In this article, we use the rate of change (ROC) as our performance indicator for determining a patient's prognosis for survival. [17] After making a forecast of overall survival, an accuracy of 0.448 was found during validation.

The primary focus of this article is tumour segmentation, both as a diagnostic aid and a precondition for treatment that relies on accurate tumour segmentation. More than one study has investigated survival prediction by combining deep learning with carefully created attributes. They used 3D U-Net to do the segmentation. [18] We first conducted preliminary experiments on a small subset of

labelled participants, and subsequently verified our results on the BraTS 2019 dataset. Another study [19] uses an ensemble of three 3D convolutional neural network models to segment the tumour region and then uses that information to derive 4524 radiomic parameters. Several methods of computing radiomic properties [20] exist, each of which accurately describes the problem at hand and aids in the resolution of a particular computer vision issue. Most researchers supplement the various machine learning and deep learning models they try to apply to the labelling problem with features they've created by hand. There is a dearth of literature devoted to the topic of enhancing machine learning algorithm performance by extracting deep features and combining them with handmade features.

3. Proposed Methodology

The proposed method is divided into three main processes for automatically segmenting tumours, extracting micro and deep characteristics, and overall survival rate of the patient based on the severity level of the glioblastoma:

1.   Data collection and preprocessing: The first step is to collect medical images (such as MRI or CT scans) and corresponding survival data of patients from a relevant database or hospital. The data should be preprocessed to remove noise, artifacts, and other unwanted features using appropriate image processing techniques.

2.   Tumor segmentation: After gathering the necessary medical images, tumour segmentation software is used to remove the tumour. This can be done using various techniques such as thresholding, region growing, active contours, or deep learning-based approaches like U-Net++, Mask R-CNN, etc.

3.   Feature extraction: Once the tumor region is segmented, both handcrafted and deep features can be extracted from the segmented region. Handcrafted features can include texture, shape, and statistical features such as mean, variance, skewness, etc. Features extracted from medical images can be improved with the use of pre-trained convolutional neural networks (CNNs) like VGG, ResNet, or Inception. With these networks, deep features can be retrieved.

4.   Survival time prediction: The final step is to predict how long a given patient will live based on the extracted attributes. Machine learning methods such as logistic regression, random forest, and support vector machine can help with this (SVMs). Some deep learning models that can be used to estimate a patient's expected lifespan are convolutional neural networks (CNNs) and recurrent neural networks (RNNs). Another kind of neural network is a recurrent neural network (RNN).

Many other metrics, such as accuracy, precision, recall,

and the F1 score, can be used to assess the proposed approach. The methodology's value can also be assessed by comparing its findings to those of alternative approaches. Two-class and three-class prediction tasks were conducted using the BraTS 2017 dataset in this experiment. When the feature matrix is complete, the following step is feature reduction so that principal component analysis (PCA) can be used to prioritise the features (PCA). Afterward, many classifiers, including Random Forest, XgBoost, SVM, and LGBM, are considered for the survival time prediction utilising each feature set separately. Then, the classifier is updated to take into account the combined information from both attributes in order to provide more accurate predictions about the patients' low, medium, and high survival rates. Figure 2 provides a visual representation of the proposed framework, and then detailed descriptions of each step are provided. In this section, we cover different approaches to tumour segmentation, feature extraction from tumour segments, and overall survival period prediction.
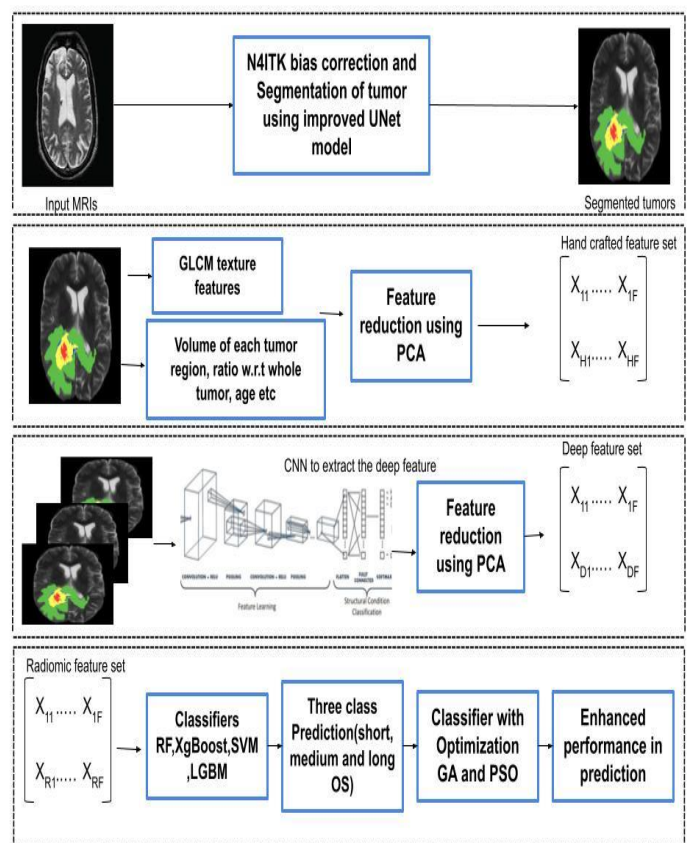

Fig 2. The proposed framework for total survival time period prediction.

a. Tumor Localization and Classification

The term "tumour segmentation" refers to the procedure of recognising and delimiting a tumour in medical imaging data like MRI, CT, or PET scans. Positron emission tomography (PET), computed tomography (CT), and magnetic resonance imaging (MRI) are just a few of the

many imaging modalities that fall under this umbrella. Accurate segmentation of a tumour is crucial for making a diagnosis, formulating a treatment strategy, and following the tumor's progression. Physical tumour segmentation is possible and is performed by radiologists; however, this procedure is time-consuming and subject to radiologists' own interpretation. Therefore, there is a growing interest in developing computer-aided tumor segmentation algorithms that can automate and standardize this task. There are various techniques used for tumor segmentation, including thresholding, region growing, edge detection, active contour models, machine learning, and deep learning.

Thresholding involves selecting a threshold value to separate the tumor from the surrounding tissue based on its intensity. Region growing involves starting with a seed point and growing the region until it reaches the tumor boundary. Edge detection techniques use gradient information to detect the tumor boundary. Active contour models use an energy minimization approach to deform a contour towards the tumor boundary. Support vector machines (SVMs) and random forests, two types of machine learning algorithms, can be trained to segment tumours using tagged data. In addition, the use of CNNs and other deep learning techniques has improved the accuracy of cancer segmentation. Tumor segmentation has numerous applications in medical imaging, including radiation therapy planning, surgical planning, and disease monitoring. Accurate tumour segmentation is a key step towards improving the precision of these applications and consequently patient outcomes. All of the tumour, necrotic areas, and augmenting areas are considered for attribute extraction in this task of tumour prediction. Data preprocessing is required for automatic tumour segmentation in order to remove biases and normalise the given MRI dataset. After that, a customised U-net model must be used for tumour segmentation.

i. Preprocessing of Data

This study's analysis was performed using data from the High Grade Glioma MRI of BraTS 2017 dataset. Artifacts in these MRIs include motion and intensity inhomogeneity, and they were acquired utilising a wide range of scanners. The algorithm and its output cannot be validated until the artefact has been removed by normalisation and bias correction. The training issue of class imbalance was overcome, and the time and memory requirements for training were much reduced, all thanks to these preprocessing processes. In a first step, median filtering is used to each patient's 3D MRI scans to reduce the amount of noise in the image by normalising the intensity of neighbouring pixels. The pictures from all modalities are then corrected using the N4ITK bias field [21, 22]. This is done to improve performance by getting rid of any artefacts that might be holding it back. In order

to account for the fact that the intensity values of the images vary from patient to patient, a normalisation phase is necessary. In this stage, the photo intensities are normalised so that they are uniform across the set. To do this, the intensity distribution is normalised such that the mean valueis close to zero and the standard deviation is close to one. As a result, the model is better equipped to generalise to new data without picking up any unwanted bias. Using the normalisation equation, where T is the original image's intensity value and μ are the mean and σ is the standard deviation of T respectively, we can write down the normalised intensity value for a given slice as:

$$T_n = \frac{T - \mu}{\sigma} \quad (1)$$

In each patient's slices, the great majority of masks were either blank or provided very little information on the tumour, making it more probable that the model would learn irrelevant background or noise rather than the tumour itself. To make sure everyone is playing on a level playing field, we set a threshold value [23] that needs at least 0.007% of the total pixels in the image to include information concerning tumours. We can now compete on an even playing field. This means that for each patient, only the picture slices containing at least 400 of the 57,600 total pixels of information about the tumour are used in the training and evaluation phases. To further reduce file size, 1% of the border was automatically cropped off all four sides of each image, resulting in a reduction in slice size from 240x240 to 192x192. These preprocessing methods not only reduced the time spent training and the amount of data stored in memory, but they also helped to address the issue of class imbalance.

The input image slice is automatically reduced in size to 192 by 192 pixels after the necessary data preparation steps have been carried out. This happens once everything that has to happen has taken place. Based on the findings of the data preparation phase, only those picture slices are used for training that include at least 0.1% of the information of the tumor's 3D volume. The dataset is comprised of 240 patients and is broken down as follows: Eighty percent are utilised for instruction, and twenty percent for evaluation: The patient data used for training totaled 170, while the patient data used for testing totaled 40. Once again, we use a random 8:2 split between training and validation data for dividing our image datasets. Information on the number of picture slices is gathered so that a model may be trained for each subtumor. After generating separate training and testing datasets for each modality, the U-Net model was used to teach the system how to distinguish between the various tumour locations. Further information on the model architecture used in this study will be provided below.

ii. Segmentation of U-Net++

When it comes to biomedical picture segmentation,

specifically tumour segmentation, the original U-Net architecture, a convolutional neural network, was constructed; this architecture's successor, U-Net++, is an expansion of the original. Another meaning for U-Net++ is "universal neural network plus." The original U-Net architecture is built upon in order to create U-Net++, which is better able to capture features across several scales and abstraction levels. It's built with extensive skip links and nesting. U-layered Net++'s skip connections allow the network to capture features functioning at varying scales by transmitting feature maps with high resolution from the encoder to the associated decoder blocks. The finer points can be preserved while the broader picture can be captured. By linking all of the feature maps from the encoder to the blocks of the relevant decoder, dense skip connections allow the network to learn a more comprehensive representation of the input. This improves the network's ability to comprehend the information it is given. The enhanced feature reuse and network-wide dissemination ultimately leads to better segmentation accuracy.

Several state-of-the-art segmentation algorithms, including U-Net itself, have been shown to be inferior to U-Net++ when it comes to the task of segmenting a wide range of biomedical images, including those with tumours. Fine-tuning the network on different datasets and applying data augmentation techniques like rotating, flipping, and scaling the data can further improve the performance of the design. U-Net++ has been shown to be effective in a number of trials, making it a viable technique for the segmentation of tumours in biomedical images. In conclusion, U-Net++ offers a robust system for disentangling images from a biological context.

Recently, the U-Net++ architecture has been put into use in cutting-edge medical applications. Like U-Net, it is a tightly supervised contraction-expansion network, but it uses a series of nested skip connections in place of the U-jump Net's interconnections between the encoder and decoder segments. Hence, it resembles U-Net quite closely yet is not identical to it. When we delve deeper into the encoder, we find not one, but four additional convolution and mixed pool levels, including a bottleneck convolution layer. After the initial encoding layer, all successive encoding levels provide a scaled-up block that is used to generate the hidden layers. Iteratively replacing them with better blocks is done until the last block's size matches that of the first.

Also, all of the nodes in this network offer skip connections to their immediate neighbours. Each convolutional layer employs a ReLu activation function [24] and a batch normalisation layer with a kernel size of to generate its final output (3, 3). Within each convolutional block is a convolutional layer, and each of these layers consists of three layers. Moreover, the

ConvTranspose layers' kernel size is set to (3, 3), strides are set to (2, 2), and padding is set to "same." For our segmentation challenge, we look at and analyse a loss function called the BCE Dice loss function (Equation 2). Just by adding the binary cross entropy to the Dice loss function, we can obtain this function. This is done so that convergence can be reached faster and overall performance can be enhanced.

$$BCE\ Dice\ Loss = \frac{2\sum_{i=1}^{n} P_i g_i}{\sum_{i=1}^{n} P_i + \sum_{i=1}^{n} g_i} + (1 - g_i)log(1 - p_i)$$
(2)

This model interacts with the U-Net++ model by trying out various pooling algorithms, which improves the model's accuracy when used to tumour segmentation. The level of similarity between the retrieved tumour parts and the real world is evaluated. The number of "survival days" is calculated based on this factor. Weighted pooling is a technique used in machine learning to summarize a set of values, giving more importance to some values than others. The Equation 3 for weighted pooling is:

$$Weighted\ pooling = (w_1 * v_1 + w_2 * v_2 + ... + w_n * v_n) / (w_1 + w_2 + ... + w_n)$$
(3)

Where v_1, v_2, ..., v_n are the values being pooled, and w_1, w_2, ..., w_n are their corresponding weights. The results of a weighted pooling calculation are the values' weighted average. In this way, the weights of the various factors can be properly considered. In other words, each value is multiplied by its weight, and the resulting products are added together. To calculate the weighted average, the sum is then divided by the total number of weights. This formula can be used for various applications, such as summarizing the scores of different features in a neural network or computing the average rating of a product based on user reviews with different weights.

To prevent overfitting caused by insufficient training images, the complete dataset is augmented with additional data. Before being utilised to build the augmented dataset, the photographs are flipped horizontally, rotated, resized, and zoomed. The model is trained with a new set of randomly combined image slices at each epoch. Algorithm 1 provides a comprehensive breakdown of the segmentation procedure.

Algorithm 1: Weighted pooling function with Tumor extraction using U-Net++

Input: M: corresponding ground truth segmentation masks.

I: Load the input MRI image data

TI: Total number of MRI images

FT: Fraction of data used for training

Output: *The final output is the segmented MRI images with the extracted tumors*

1. *normalize I with N41TK bias normalization*

2. *Reform I, M is to 240×240 Pixel size of cropping boundary regions*

3. *IF Brain Tumor = Complete do:*

4. *Then Return Mask*

5. *IF Brain Tumor = NECROTIC do:*

6. *Then Return Mask*

7. *IF Brain Tumor = ENHANCING do:*

8. *Then Return Mask*

9. *Training: Train the model using the augmented dataset and binary cross-entropy loss. Optimize model parameters using the Adam optimizer*

10. *Evaluation: Evaluate the trained model using the validation dataset to measure segmentation performance*

11. *Testing: Segment tumors in the test dataset using the trained model*

12. *For NE epochs do:*

13. *Update U-Net++ weights*

14. *Prediction ← Predict Segmented Mask for MRI images shape*

15. *Extracted Brain Tumor ← Image Shapes * Prediction*

b. Feature Extraction

Feature extraction in survival prediction for glioblastoma multiforme (GBM) using radiomic features is a method for identifying and quantifying imaging biomarkers from medical images that can predict patient survival. Here's an overview of the algorithm:

1. Image acquisition: Collect and pre-process magnetic resonance (MR) images of patients with GBM.

2. Region of interest (ROI) segmentation: Segment the tumor region using manual or automated methods.

3. Feature extraction: Extract radiomic features from the segmented tumor region using feature extraction methods. These features may include shape, texture, intensity, and gradient features.

4. Feature selection: Select the most important features using statistical or machine learning-based feature selection methods.

5. Survival prediction model: Train a survival prediction model using the selected radiomic features and the survival time of each patient. The model can be a Cox proportional hazards model, a random survival forest, or another survival analysis method.

6. Model evaluation: Evaluate the trained model's performance using a validation dataset, measuring the model's accuracy, sensitivity, and specificity.

7. Testing: Apply the trained model to a new set of MR images to predict survival times.

8. Clinical translation: Translate the radiomic features and the trained model into a clinically useful tool for survival prediction in GBM patients.

The segmented ROI is the source of the handcrafted elements employed in this work. Although the human-created features characterise the projected tumor's texture and shape, the deep features take characteristics from the input using a convolutional operation, providing a response critical to the model's ultimate output. This research employed the recovered ROI segment to identify the artisanal qualities. In order to determine the volumes of the entire tumour, the necrotic portion, and the augmenting portion, all of the relevant pixel values are added up. To further understand the tumor's structure, its perimeter is calculated at several levels. The texture features that are produced by the grey level co-occurrence matrix have also been considered (GLCM). Here, we offer a strategy for extracting the texture's second-order statistical features from a sample of image pixels. [25] One of the numerous potential uses of GLCM in the field of medical image processing is the analysis of fine-grained texture data. Hence, 12 features, one each from the tumor's location, size, and grade, are considered. Six other factors in addition to incidence and energy are considered when employing GLCM.

Each segmented portion of the tumour is characterised by six different characteristics. Maximum and minimum pixel values, mean and standard deviation, area, perimeter, and volume are all part of this set of statistics. We employ the patient's age feature from the dataset in conjunction with a total of 12 created characteristics to accomplish the classification objective. Deep features, also known as network-generated features, are features that are developed in response to a task by the networks themselves. More complicated input patterns, such as textures, forms, or versions of previously processed features, can be handled by the "deeper" layers of a deep learning model's ability to learn and produce its own feature filters. The "deeper" layers can then use this information to learn how to handle increasingly complex inputs. Specifically, we apply the technique of reinforcement learning to reach our goal.

One of the most often used deep models for the various medical imaging-related applications is convolutional neural networks [26, 27]. The CNN representation depicted in Figure 3 has been our primary model of choice when computing deep features. When CT, ET, and NT are separated, the data is stacked to create 128 by 128 by 3 dimensions before being fed into the CNN model. The model consists of a layer for data flattening and three layers for convolutional processing. Each convolutional layer appends a three-by-three-dimensional kernel to the input data, together with an equal amount of padding, resulting in a single complicated feature map. Two-by-two pools are the maximum allowed for pooling purposes. The output of a CNN's flatten layer is often taken as a proxy for the network's deep feature matrix. After running the model, we obtain an estimated total of 5120 deep features.
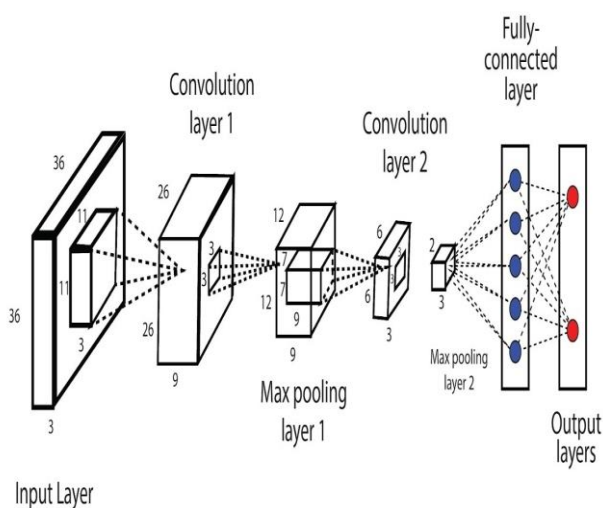

Fig 3. Architecture of Deep CNN for feature extraction

i. Fusion of features and Feature reduction using PCA

Principal component analysis (PCA) can be used to decrease the dimensionality of a dataset, while combining features can improve the accuracy with which machine learning models classify data. These two methods both use feature reduction. Follow these guidelines when implementing any of these methods. The term "PCA" refers to the statistical method known as principal component analysis, which reduces a dataset's unique characteristics to a smaller number of linearly independent variables. The dimensionality of the dataset can be reduced using this method. Each of these key components is responsible for describing a certain amount of the overall variance in the dataset, and this variance is used to rank them from most to least important. To reduce the number of features in a dataset without losing sight of the most important information, principal component analysis (PCA) can be used. Feature dimensions for both the manually constructed features and the CNN model-generated features can be reduced using principal component analysis (PCA). The combined benefits of

these two approaches are substantial. When dealing with massive datasets, principal component analysis (PCA) [28] is often used since it reduces the number of dimensions without losing too much information.

The purpose of the method known as "feature fusion" is to improve classification precision by merging different types of features gathered from the same or other datasets. The most common fusion techniques include early, late, and hybrid fusion. Early fusion combines features at the input level before the model's processing, late fusion combines the predictions of multiple models, and hybrid fusion combines the features at the input level and the models' predictions. Although there is a correlation between NCSV and the number of major components, it has been demonstrated that 96% of the cumulative variance can be kept with just eight specially chosen features. As NCSV is inversely proportional to the number of principal components, this was theoretically feasible. A closer look at the graph proves the validity of this assertion. Similarly, [22] deep characteristics have been selected as the primary features to use while classifying data. These 30 features are utilised to make a prediction, and several trials showed that a minimum of 9 features was sufficient for an accurate prediction to be made (8 fused features plus age). These feature matrices are used as an input by several distinct machine learning algorithms employed in the larger survival prediction task.

c. Prediction of overall survival period

Predicting overall survival (OS) period in medical applications, such as cancer prognosis, is a crucial task that can aid in the development of personalized treatments and improve patient outcomes. Machine learning algorithms, such as regression and survival analysis models, can be used to predict OS based on clinical and molecular features. Collect clinical and molecular data from patients, including demographic information, clinical measurements, biomarker expression levels, and genomic profiles. Preprocess the data by normalizing, scaling, and imputing missing values. Select relevant features using statistical tests, feature ranking methods, or domain expertise. Extract additional features using dimensionality reduction techniques, such as principal component analysis (PCA) or feature fusion. Use the trained model to predict OS for new patients based on their clinical and molecular features. Deploy the model in a clinical setting by integrating it into a decision support system or electronic health record.

In this article, Algorithm 2 discusses the forecasting method in greater depth. A brief summary of the following is provided in the next paragraph: Support vector machines (SVMs), random forests (RFs), linear boosting machines (LBMs), and xgBoost are the four machine learning techniques used for operating system prediction.

Machine learning methods are combined with bio-inspired optimisation algorithms to further enhance the final product. In order to illustrate the effectiveness of the optimisation technique, the authors of this work consider the genetic algorithm and the PSO. This allows the algorithms to quickly filter out irrelevant characteristics and focus on those that have promise. Because of this, GA and PSO can provide comparable performance to traditional approaches while taking a lot less time to implement. "SVM," short for "support vector machine," are a form of method that is computationally costly, robust, and accurate [29,30]. The possibility for good results exists even with little amounts of training data. The Random Forest algorithm is an ensemble approach that uses several decision trees to reach a single conclusion.

The shape of the woods provided the inspiration for the name. Due to its accuracy and speed when applied to huge datasets, it has become one of the most used machine learning algorithms [31,32]. This is because it is one of the most widely used machine learning algorithms. Lite GBM is an efficient and scalable method of gradient boosting [33,34]. It employs decision trees similar to those in Random Forest. It differs from other boosting algorithms in that it employs the best fit approach while splitting the tree. This technique trains swiftly and efficiently, while using far less memory than competing methods. This has resulted in the algorithm's widespread use. As an alternative to LGBM, XgBoost [35,36], a gradient boosting decision tree approach, may be able to deal with parallel tree boosting in a similar fashion (such as GBDT and GBM).As a result of its high precision and negligible impact on resources like CPU time and RAM, the method has gained significant use.

Algorithm 2: *Survival days Prediction using PCA and radiomic features*

Input: *ET : Extracted Brain Tumor Region*

    TS : Total number of Slices in each MRI image = 256

    FT : Fraction of total Slice to be taken

    NC1 : Number of Components for PCA1

    NC2 : Number of Components for PCA2

Output: *The final output is the survival days of each patient from survival rate*

1.   Collect a dataset of patients with known survival times and radiomic features extracted from their medical images.

2.   For I   ← 0 to N do:

3.   Compute volume = sum of tumor pixels

4.   Divide the data into two groups: a training set and a test set.

5.   ET   ← complete append, necrotic and enhancing ET in RGB fashion

*6.   ET   ← extract TS * FT slices having Brain tumor region*

7.   If necessary, apply PCA to the radiomic features to reduce the dimensionality of the data

8.   Standardize the data to have a mean of 0 and a standard deviation of 1

9.   Compute deep features of OT by CNN flatten layers

10.   PCA1   ← apply PCA to deep features with components = N1

11.   PCA2   ← apply PCA to deep features with components = N2

12.   X   ← Append PCA1, PCA2

13.   Train a machine learning algorithm, such as linear regression, logistic regression, or support vector machines, on the training set using the radiomic features as input.

14.   Train models of X-train, Y-train

15.   Evaluate the performance of the algorithm on the testing set using metrics such as the mean squared error, the area under the ROC curve, or the concordance index.

---

4. Experimental Result Analysis

U-Net++ was used to carry out the proposed segmentation for the BraTS 2017 dataset, and many classifiers, including SVM, Random Forest, Light GBM, and XgBoost, were put to use for prediction. We validated and evaluated these processes. The test is run on a Windows 10 PC with 4 GB of RAM, a Google Collaborator platform, an Nvidia Tesla GPU back end, and the latest version of the Tesla graphics processing unit driver. The ages of patients and their overall survival rates are both included in this dataset (OS). A total of 163 patients are split in two: the first 80 are utilised for training, while the second 20 are used for evaluation. An additional 8:2 split is made between the training and validation halves of the dataset.

With the data preprocessing steps completed as described earlier, the input image slice's original 240 by 240 pixel resolution will be automatically decreased to 192 by 192. Metrics37 that are widely accepted as helpful for image segmentation are used to assess the segmentation's

effectiveness. Several criteria such as sensitivity, specificity, F1 score, Dice score, and accuracy are used. An algorithm's efficacy can be demonstrated with a confusion matrix, and the matrix can also be used to calculate segmentation and classification accuracy. The TP, FP, FN, and TN values of these matrices can each be represented by one of the four possible entries. All of the sub-tumor segmentations' confusion matrices are generated during training. The purpose of doing this is to improve the model's precision.

Each of the aforementioned measures of efficiency has been defined below:

- The following is a definition of accuracy (equation 4):

$$Accuracy = (Number\ of\ Correct\ Predictions) / (Total\ Number\ of\ Predictions) \qquad (4)$$

- In order to get the genuine negative rate, or specificity, we use equation 5 to determine the percentage of non-tumor class pixels that were accurately recognised.

$$Specificity = True\ Negatives / (True\ Negatives + False\ Positives) \qquad (5)$$

- Sensitivity is a metric that evaluates at the proportion of foregrounds that were correctly predicted. In other contexts, the term "recall" may be used instead. It shows (with the help of Equation 6) what percentage of the background was accurately predicted.

$$Sensitivity = True\ Positives / (True\ Positives + False\ Negatives) \qquad (6)$$

- The F1-score, defined in Equation 7, is a common metric used to categorise different types of imbalance. You can read about it in terms of Precision and Recall.

$$F1\ Score = 2 * (Precision * Recall) / (Precision + Recall) \qquad (7)$$

a. Brain Tumor Segmentation Results

The success of the suggested technique hinges on the accuracy with which an area of interest can be retrieved from MR images. Several "modalities" of magnetic resonance imaging (MRI) disclose different intrinsic features of the tumour portion. The algorithm utilised to compute the features is decided based on the essential properties of the tumour subregion. T1-weighted contrast-enhanced (T1ce) imaging is useful for highlighting tumour features and removing necrotic ones [19]. When compared to other imaging modalities, a high intensity signal in T1ce implies a high-intensity region, therefore this is made achievable. For comprehensive tumour segmentation, the T2 weighted modality is used. The

segmentation outcomes are presented in Table 1. The significant improvement in precision was made possible by the U-Net++ model, which makes use of a weighted pooling function. Overall, our tumour segmentation accuracy was 98.76%, tumour enhancement segmentation was 99.15%, and necrotic tumour region segmentation was 99.21%.

Brain tumour segmentation is a crucial aspect of medical image processing that helps doctors pinpoint the exact location of tumours in the brain and assess their size. Several measures can be used to assess the efficacy of brain tumour segmentation such as:

- Dice coefficient: evaluates how much the ground-truth tumour region overlaps with the segmented tumour region.

- Jaccard index: evaluates how closely the segmented cancer region matches the ground truth tumour region.

- Sensitivity and specificity: examines how effectively the segmentation method can tell the difference between false-positive and false-negative occurrences.

- Positive predictive value (PPV) and negative predictive value (NPV): provides an estimate of the proportion of "true positive" and "true negative" cases relative to the total number of positive and negative samples.

The performance of brain tumor segmentation methods can vary depending on various factors such as the imaging modality used (e.g. MRI, CT), the type and location of the tumor, the quality of the images, and the segmentation algorithm used. Deep learning-based methods, such as U-Net and Mask R-CNN, have shown promising results in brain tumor segmentation, achieving high dice coefficients and Jaccard indices.

Using the BraTS 2017 dataset, Figure 4 displays a few visual segmentation results for HGG patients. Both the expected tumour subregions and the ground-truth picture are shown in this diagram. Many patients' original T1ce and T2 MRI slices are shown on the left, each with a unique volume of tumour in the axial plane that is connected to the ground. In reality, the whole tumour is a beautiful shade of blue, while the necrotic subtumor is depicted in red and the promoting part of the tumour is shown in yellow. There are 192 minute parts that make up each picture. Third, fourth, and fifth rows on the 2D plane, respectively, display the segmented enhancing volume, the total necrotic volume, and the overall volume of the tumour. Thanks to the images, we can easily make sense of how the experimental findings relate to the real world. The volume of the segmented tumour part is comparable to the volume of the original tumour, and this is reflected in the many metrics used to measure it.

Sub parts of Brain tumor	Accuracy	Specificity	Sensitivity	F1 Score
Complete brain tumor	0.992	0.997	0.867	0.943
Enhancing brain tumor	0.991	0.999	0.805	0.933
Necrotic brain tumor	0.987	0.998	0.671	0.932

Table 1. The results of tumour segmentation with the proposed U-Net++ algorithm for various MRI modalities
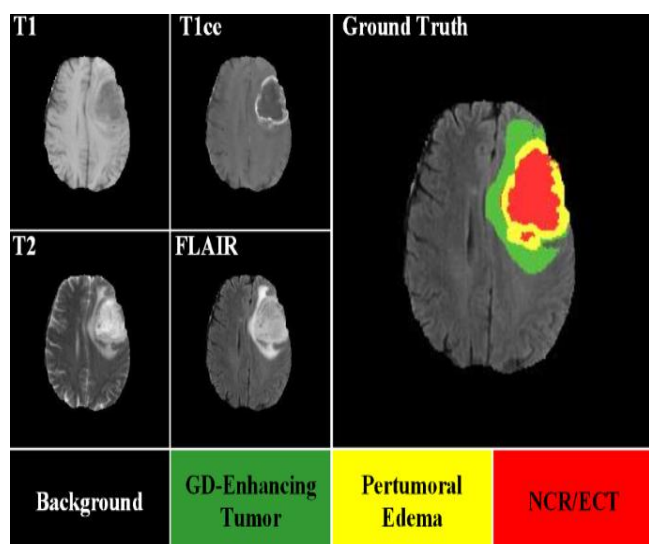

Fig 4. The visual results of segmenting augmenting, necrotic, and complete tumours, along with the corresponding ground truths

b. Results Prediction

After the tumours have been segmented from the original MRI scans, the same methods used in computing the deep features and the produced features can be applied. The term "survival" refers to the time a patient spends alive after receiving a pathology diagnosis and before dying. All 163 patients are used in the prediction task, with each patient's survival days being assigned to one of three groups at various points in the surgical process. Procedures performed on the two groups that made it through the experiment are as follows:

• hree class survival group: People are divided into long-term survivors, short-term survivors, and those who have survived for an interval period of time. Those who have managed to hang on for longer than 15 months are considered long-survivors. People with short survival times have been alive for fewer than ten months (survive period between 10 and 15 months).

• Two class survival group: As evidenced by the existence of both long-term survivors (those who have made it this far after more than a year) and short-term survivors (those who have made it this far after a year or less), the zombie apocalypse left behind a diverse group of victims (survive period less than 12 months). The duration of this period is determined by examining the median amount of life and labour represented in the data set.

For the first stage, we employ SVM, RF, LGBM, and XgBoost alongside a total of 37 handcrafted features. The prognosis for the patient can then be categorised accordingly. As such, the survival day's projection makes use of all 5120 estimated deep qualities independently. Classification was performed for both the 2 and 3 class survival groups, and comparisons were made using the stated reference measures in Tables 2 and 3. In comparison, the best results you can get out of XgBoost include a 3-class group classification, where it achieves an F1 score of 56% and an accuracy of 59%. SVM's best results from manually produced features are 59% accuracy and 53% F1 score. For two-class classification, LGBM's highest accuracy is 68% and F1 score is 67% when using manually built features. In contrast, when deep features are used, both Support Vector Machines and Random Forest achieve 66% accuracy, with RF having a slightly higher F1 score. The research also calculates the area under the curve (AUC value) and compares the ROC curve performance to the TP rate to assess the pixel classification performance. Also, the TP success rate is compared to the ROC curve's performance. The area under the curve (AUC) is a common statistic used to evaluate the efficacy of various classifiers. As AUC rises, segmentation and classification accuracy improves. We found that when classifying data into three categories, we could get an AUC of up to 69% and 70% throughout the experiment using handcrafted and deep features, respectively; however, while classifying data into two categories, we could only achieve an AUC of up to 68% and 66%, respectively.

You can see the outcomes in Tables 2 and 3, and they indicate that the accuracy of manually constructed features is better than that of deep features when used alone. Features that take into account a person's age are among the most valuable ones you can make for a categorization process. By incorporating deep features, however, the CNN model itself is tasked with computing the features in question. The convolutional and max pooling techniques help with this. Hence, we have employed the radiomic features, which are the best features fused from both feature sets, and conducted trials to see how well they

predict the survival group. We performed a series of experiments with the aim of identifying the most effective features to utilize, and we discovered that using a total of nine features—eight radiomic variables and one that is the age that is provided in the dataset—gave us the greatest results.

In order to choose the features shown here, the PCA algorithm is employed, which was previously described. Table 4 shows the outcomes of using radiomic qualities to categorise survival groups into three groups, while table 5 shows the outcomes of using radiomic characteristics to categorise survival groups into two groups. To ensure the categorization approach is reliable, a five-fold cross validation is performed. Using XgBoost to three-class classification results in an accuracy of 62% and an AUC of 73%, much outperforming alternative approaches. After this change, the classification's efficiency increased by 4%. By using the LGBM algorithm, we can raise the accuracy by 6% and the AUC by 73% when classifying data into two groups.

Prediction performance of survival rate (three classes)			
SVM	Random Forest	XgBoost	LGBM
Accuracy (in %)			
features Hand crafted			
0.5714	0.5058	0.5141	0.5206
Deep features			
0.5434	0.5790	0.5450	0.5242
Sensitivity			
features Hand crafted			
0.5161	0.5390	0.5321	0.5317
Deep features			
0.5001	0.5122	0.5451	0.5728
Specificity			
features Hand crafted			
0.5577	0.5651	0.5533	0.5939
Deep features			
0.5140	0.5806	0.5285	0.5114
F1 score			
features Hand crafted			
0.5396	0.5396	0.5986	0.5309
Deep features			
0.4781	0.4522	0.5012	0.5621
ROC (AUC)			
features Hand crafted			
0.5001	0.5938	0.5985	0.5973
Deep features			
0.5680	0.5805	0.5939	0.6192

Table 2. Survival rate predictions for BraTS 2017, separated into three groups (low, medium, and high) based on the use of both hand-crafted features and deep features.

Prediction performance of survival rate (two classes)			
SVM	Random Forest	XgBoost	LGBM
Accuracy (in %)			
features Hand crafted			
0.6818	0.6642	0.6518	0.6267
Deep features			
0.6151	0.6642	0.6649	0.6528
Sensitivity			
features Hand crafted			
0.6580	0.8066	0.6458	0.5852
Deep features			
0.6727	0.6117	0.6617	0.6227
Specificity			
feature			
0.703	0.5183	0.6558	0.668

s Hand crafted	6			3
Deep features	0.5573	0.7161	0.6698	0.6838
F1 score				
features Hand crafted	0.6788	0.6521	0.6472	0.6247
Deep features	0.6119	0.6596	0.6606	0.6481
ROC (AUC)				
features Hand crafted	0.6808	0.6625	0.6507	0.6268
Deep features	0.6150	0.6639	0.6658	0.6533

Table 3. Predictions of survival rates for BraTS 2017 are split into two groups (low and high) based on the use of hand-crafted features and deep features.

	SVM	Random Forest	XgBoost	LGBM
Accuracy (in %)				
Average	0.6041	0.5902	0.5926	0.6261
standard deviation σ (SD)	2.23	2.5	2.32	2.21
Sensitivity				
Average	0.4794	0.4306	0.4607	0.5114
standard deviation σ (SD)	2.7	2.1	2.81	2.82
Specificity				
Average	0.5174	0.5641	0.5387	0.5129
standard deviation	2.81	3.21	2.73	3.1

deviation σ (SD)				
F1 score				
Average	0.4706	0.3612	0.4170	0.5072
standard deviation σ (SD)	2.4	2.56	2.21	2.1
ROC (AUC)				
Average	0.6132	0.5778	0.6024	0.6363
standard deviation σ (SD)	3.11	3.3	3.21	3.12

Table 4. Survival rate prediction using proposed radiomic characteristics for BraTS 2017: mean and standard deviation from five separate runs (σ [SD]) three groups of survivors were identified by a different radiomic feature.

Figure 5 shows how ROC curves were built to verify the quality of results received from different radiomic feature classifiers. A genetic algorithm is a type of optimization search method; it is built to enhance search efficiency even for difficult problems, and it does so without requiring any kind of local optimal solution. [32] Each solution in a GA is updated over time as the population evolves under the guidance of a fitness function to achieve population optimization. We go to such lengths to ensure the highest quality outcomes. Particle swarm optimization (PSO), another bio-inspired optimization method, is employed to compare the results. Using an iterative process that compares a potential solution to one that has already been optimized, PSO can locate the best option.

In this study, we combine these two optimisation procedures with a machine learning-based strategy to enhance the accuracy of our survival prediction model. Each of SVM-GA, LGBM-GA, XgBoost-GA, and RF-GA, as well as SVM-PSO, LGBM-PSO, XgBoost-PSO, and RF-PSO, are evaluated for their performance. Here, we use genetic algorithms and particle swarm optimisation to maximise the accuracy of our forecasts in accordance with a predetermined set of standards. As can be shown in Table 6, the GA method outperforms PSO in the 3-class survival group, whereas PSO offers more accurate results in the 2-class classification. With the RF-Fused feature-GA method, the proposed scheme's accuracy went up from

59% to 67%, and the AUC went up from 69% to 74%, both for 3-class survival classification. Using the Lite GBM-Fused feature-PSO method to the 2-class survival group classification increases accuracy from 68% to 79% and area under the receiver operating characteristic curve (AUC) from 68% to 80%.
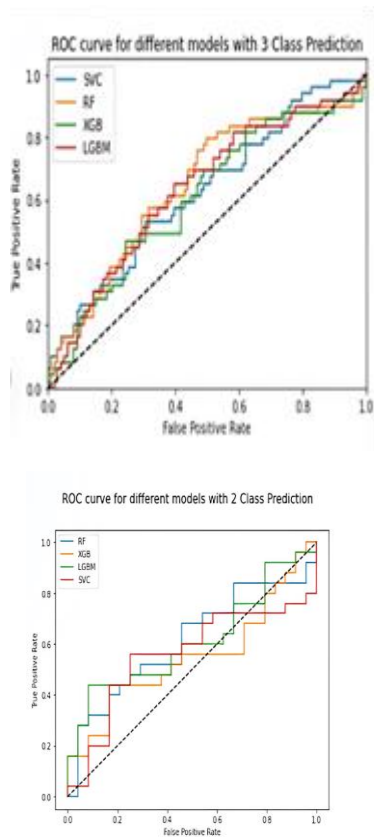

Fig 5. ROC Curves for different models with 3 class and 2 class prediction

	SVM	Random Forest	XgBoost	LGBM
Accuracy (in %)				
Average	0.7041	0.6902	0.6926	0.7261
standard deviation σ (SD)	3.22	3.5	3.34	3.25
Sensitivity				
Average	0.5794	0.5306	0.5607	0.6114
standard deviation σ (SD)	3.7	3.1	3.83	3.85
Specificity				
Average	0.6174	0.6641	0.6387	0.6129
standard deviation σ (SD)	3.82	4.25	3.76	4.1
F1 score				
Average	0.5706	0.4612	0.5170	0.6072
standard deviation σ (SD)	3.4	3.54	3.23	3.1
ROC (AUC)				
Average	0.7132	0.6778	0.7024	0.7363
standard deviation σ (SD)	4.12	4.3	4.25	4.18

Table 5. The average and standard deviation of the results from five separate iterations of a survival rate prediction model using the proposed radiomic properties for BraTS 2017 (σ [SD]).

c. Statistical Analysis

Table 7 displays the results of a statistical analysis performed using the ANOVA test, where the area under the curve (ROC) value is considered and the significance level (α) is set to 0.05. To be more specific, the null hypothesis claims that the results obtained by multiple machine learning algorithms using different sets of characteristics are not significantly different from one another. That's in contrast to the competing theory, which posits a very sizable variation. Each of these requirements must be met before we can accept that this hypothesis is true. The larger p-value in this case (0.370986762 for 3-class and 0.942262483 for 2-class) shows that there is little to no difference in the performance of the three strategies, making the suggested survival prediction generalised and algorithm-agnostic. Again, the fact that the p-value for 2-class is greater shows that the overall performance of the various approaches is virtually same. In a similar vein, the study is performed to learn how the attributes impact the reliability of the forecast. It was determined that the p-value for the 3-class was

0.172210523, and that for the 2-class it was 0.187646728. While this may imply that there is not a huge difference between the feature sets, the fact that the significance level was slightly above 0.05 shows that it does effect performance.

Another statistic that evaluates the prognosis's accuracy in a clinical setting is the diagnostic odds ratio (DOR). The utility of a diagnostic test can be calculated with its help. [38] The probability of a positive test result for a given class can be defined as the ratio of the probabilities of a positive result for that class to the probabilities of a negative result for that class. To put it another way, it assesses the likelihood of a favorable result in each scenario. Equation 8 shows that DOR's specificity and sensitivity are independent variables (8). A DOR greater than 1 indicates a more successful test, while a DOR less than 1 suggests the technique should be improved. The results of the provided approach cannot be inferred from the fact that the DOR value is one. Whole tumour extraction has a DOR of 1269.29 CT, improved tumour extraction of 2033.99, and necrotic tumour extraction of 648.00 for the segmentation job. The tumor's modest and complete spread makes is difficult to distinguish the necrotic area from the remainder of the tumour. Using fused features for a 2-class classification, the LGBM classifier's maximum DOR value is equal to 2.9595. The current value, obtained using XgBoost's 3-class classifier, is 1.1201. Predicting the overall survival rate is helpful in the clinic, as indicated by the number, but doing so remains a challenge for scientists due to the wide variation in tumour types and patient overall survival.

$$Diagnostic\ odds\ ratio\ (DOR) = \frac{Sensitivity \times Specificity}{1-sensitivity \times 1-Specificity}$$
(8)

Table 6. Optimization algorithm and the median survival rate prediction using fused features in a 5-fold cross-validation study

	SVM	Random Forest	XgBoost	LGBM
Genetic algorithm (%)				
Two classes prediction				
Accuracy (in %)	0.7508	0.7575	0.7843	0.7524
F1 Score (AUC)	0.7667	0.75	0.7772	0.7481
ROC	0.7675	0.7554	0.7791	0.7508
Three class prediction				
Accuracy (in %)	0.7407	0.7124	0.6719	0.6234
F1 Score (AUC)	0.6116	0.5355	0.6123	0.5922
ROC	0.7403	0.707	0.7492	0.726
Optimization of PSO (%)				
Two classes prediction				
Accuracy (in %)	0.7363	0.7969	0.7363	0.7363
F1 Score (AUC)	0.736	0.7966	0.7278	0.736
ROC	0.7388	0.8	0.7277	0.7388
Three class prediction				
Accuracy (in %)	0.6102	0.5855	0.5731	0.604
F1 Score (AUC)	0.5857	0.4996	0.4466	0.5364
ROC	0.726	0.677	0.6547	0.7034

Table 7. Analysis of the p-value (significance level = 0.05) significance level of the impact of various factors on the prediction of survival days and Effect of different algorithm

Features / Algorithm	Features Hand crafted	Deep features	Radiomic features	p-value (α= 0.05)
prediction of Three Class survival				
SVM	0.5985	0.589	0.6324	0.1722105
Random Forest	0.5985	0.5978	0.6143	
XgBoost	0.5974	0.6456	0.6879	
LGBM	0.6745	0.657	0.7234	
p-value (α= 0.05)	0.3709868			
prediction of two Class survival				
SVM	0.5873	0.5879	0.5764	0.1876467
Random Forest	0.5786	0.5987	0.6234	
XgBoost	0.5768	0.5723	0.6287	
LGBM	0.5908	0.5654	0.6983	
p-value (α= 0.05)	0.9422625			

5. Conclusion

This article delves into the topic of how many days on average an HGG person can expect to survive for. If the brain tumour is successfully segmented, then this prognosis will be accurate. The proposed method starts with an initial period of time spent on preparing the data. When applied to a collection of MRI scans from different locations, this method helps standardise the pixel intensities. Spending less on computers is another

benefit of this technique. Both the deep features computed by CNN and the manually produced attributes, such as texture and volume, are extracted from the segmented parts of the tumour. Hence, tumour segmentation is a crucial stage [39,40] that needs to be completed prior to feature extraction, and the efficiency of survival rate prediction is dependent on the accuracy of the segmentation. The ability of deep models to automatically extract essential characteristics from the data using highly effective convolutional and pooling operations has given them a significant advantage on their more traditional ones in a number of medical imaging applications. Getting an F1score reveals how precise the segmentation performed. Then, the prediction task is executed taking the feature extraction, the deep features, and the integrated radiomic characteristics into account, and the performance is thoroughly investigated. The purpose of using principal component analysis (PCA) during merging is to reduce the number of dimensions in order to select those that yield the maximum accuracy with the lowest increase in computational cost. By using a wide variety of machine learning algorithms for prediction, the proposed method has been improved and made algorithm independent. These algorithms include RF, SVM, LGBM, and XgBoost. Algorithm independence in terms of the scheme's accuracy is further demonstrated through statistical analysis. The model's superior performance is a result of the bio-inspired optimisation algorithm's combination of the inherent extraction of deep features with more conventional, hand-crafted features. But nevertheless, due to the limited number of individuals available at this time, there is a great deal of space for investigation and improvement of the survival days forecast. Adding a large dataset for performance and robustness verification, as well as a cutting-edge deep learning methodology for classification, would be great steps forward for this strategy.

Conflict of Interest

The authors declare that they have no conflict of interest. The manuscript was written through contributions of all authors. All authors have given approval to the final version of the manuscript.

Data Availability Statement

Data sharing not applicable to this article as no datasets were generated during the current study.

Ethics approval

This article does not contain any studies with human participants performed by any of the authors.

Consent to Participate

Not applicable.

Funding details

None.

Informed Consent

All the authors well aware submission of manuscript.

References

[1] G. B. Janardhana Swamy, Anusha, Lavanya, Meghashree, and Sangeetha, "Brain tumor detection using convolutional neural network," International Journal for Research in Applied Science and Engineering Technology, vol. 8, no. VI, 2020.

[2] D. Dheeraj and H. S. Prasantha, "Study of machine learning vs. deep learning algorithms for detection of tumor in human brain," International Journal of Computer Science and Engineering, vol. 8, no. 1, pp. 2347–2693, 2020

[3] Nader D, Jehlol H, Subhi A, Oleiwi A. Brain tumor detection using shape features and machine learning algorithm. Int J Sci Eng Res. 2015;6(12):454-459.

[4] Louis DN, Perry A, Reifenberger G, von Deimling A, Figarella-Branger D, Cavenee WK. The 2016 World Health Organization classification of tumors of the central nervous system: a summary. Acta Neuropathol. 2016;131(6):803-820. https://doi.org/10.1007/s00401-016-1545-1

[5] Dong H, Yang G, Liu F,Mo Y, Guo Y. Automatic brain tumor detection and segmentation using U-Net based fully convolutional networks. Paper presented at: Proceedings of the Annual Conference on Medical Image Understanding and Analysis; 2017:506-517; Springer, Cham.

[6] Guo X, Yang C, Lam PL, Woo PYM, Yuan Y. Domain knowledge based brain tumor segmentation and overall survival prediction. In: Crimi A, Bakas S, eds. Brainlesion: Glioma, Multiple Sclerosis, Stroke and Traumatic Brain Injuries. BrainLes 2019. Lecture Notes in Computer Science. Vol 11993. Cham, Switzerland: Springer; 2020. https://doi.org/10.1007/978-3-030-46643-5_28

[7] Rajinikanth V, Satapathy SC, Fernandes SL, Nachiappan S. Entropy based segmentation of tumor from brain MR images – a study with teaching learning based optimization. Pattern Recogn Lett. 2017;94(2017):87-95. https://doi.org/10.1016/j.patrec.2017.05.028

[8] Rajinikanth V, Fernandes SL, Bhushan B, Harisha SNR. Segmentation and analysis of brain tumor using Tsallis entropy and regularised level set. In: Satapathy S, Bhateja V, Chowdary P, Chakravarthy V, Anguera J, eds. Proceedings of the 2nd International Conference on Micro-Electronics, Electromagnetics and Telecommunications. Lecture

Notes in Computer Science. Vol 434. Singapore: Springer; 2018. https://doi.org/10.1007/978-981-10-4280-5_33

[9] Menze B, ReyesM, van LeemputK. Themultimodal brain tumorimage segmentation benchmark (BraTS).IEEE TransMedImaging. 2015;34(10):1993-2024.

[10] Hanif F, Muzaffar K, Perveen K, Malhi SM, Simjee SU (2017) Glioblastoma multiforme: a review of its epidemiology and pathogenesis through clinical presentation and treatment. Asian Pac J Cancer Prev 18:3–9. https://doi.org/10.22034/APJCP.2017.18.1.3

[11] Fernandes SL, Tanik UJ, Rajinikanth V, et al. A reliable framework for accurate brain image examination and treatment planning based on early diagnosis support for clinicians. Neural Comput Appl. 2020;32:15897-15908. https://doi.org/10.1007/s00521-019-04369-5

[12] Amin J, Sharif M, Yasmin M, et al. A new approach for brain tumor segmentation and classification based on score level fusion using transfer learning. J Med Syst. 2019;43:326. https://doi.org/10.1007/s10916-019-1453-8

[13] Das S. Brain tumor segmentation from MRI images using deep learning framework. Advances in Intelligent Systems and Computing Book Series (AISC). Vol 1119. Singapore: Springer; 2020:105-114.

[14] Das S, Swain MK, Nayak GK, Saxena S. Brain tumor segmentation from 3D MRI slices using cascading convolutional neural network. In: Advances in Electronics Communication and Computing. Singapore: Springer; 2021:119-126.

[15] Munivara Prasad, K., Samba Siva, V., Krishna Kishore, P., Sreenivasulu, M. (2019). DITFEC: Drift Identification in Traffic-Flow Streams for DDoS Attack Defense Through Ensemble Classifier. In: Peng, SL., Dey, N., Bundele, M. (eds) Computing and Network Sustainability. Lecture Notes in Networks and Systems, vol 75. Springer, Singapore. https://doi.org/10.1007/978-981-13-7150-9_32

[16] Acharya UR, Fernandes SL,WeiKoh JE, et al. Automated detection of Alzheimer's disease using brainMRI images – a study with various feature extraction techniques. J Med Syst. 2019;43:302. https://doi.org/10.1007/s10916-019-1428-9

[17] Yang D, Rao G, Martinez J, Veeraraghavan A, Rao A. Evaluation of tumor-derived MRI-texture features for discrimination of molecular subtypes and prediction of 12-month survival status in glioblastoma. Med Phys. 2015;42(11):6725-6735. https://doi.org/10.1118/1.4934373

[18] Palsson S, Cerri S, Dittadi A, Leemput KV. Semi-supervised variational autoencoder for survival prediction. Lecture notes in computer science (including subseries lecture notes in artificial intelligence and lecture notes in bioinformatics); 2020: 11993 LNCS, 124–134. arXiv:1910.04488.

[19] Sun L, Zhang S, Chen H, Luo L. Brain tumor segmentation and survival prediction using multimodal MRI scans with deep learning. Front Neurosci. 2019;13:1-9.

[20] Zhou M, Scott J, Chaudhury B, et al. Radiomics in brain tumor: image assessment, quantitative feature descriptors, and machine-learning approaches. Am J Neuroradiol. 2018;39:208-216.

[21] P. Krishna Kishore, S. Ramamoorthy, V.N. Rajavarman, ARTP: Anomaly based real time prevention of Distributed Denial of Service attacks on the web using machine learning approach, International Journal of Intelligent Networks, Volume 4, 2023, Pages 38-45, ISSN 2666-6030,https://doi.org/10.1016/j.ijin.2022.12.001.

[22] Song S, Zheng Y, He Y. A review of methods for bias correction in medical images. Biomed Eng Rev. 2017;1(1):1–10. https://doi.org/10.18103/bme.v3i1.1550

[23] Bennaceurab M, Saoulia R, Akilb M, Kachourib R. Fully automatic brain tumor segmentation using end-to-end incremental deep neural networks in MRI images. Comput Methods Progr Biomed. 2018;166:39-49.

[24] Nwankpa CE, Ijomah W, Gachagan A, Marshall S. Activation functions: comparison of trends in practice and research for deep learning; 2018. arXiv:1811.03378.

[25] Mall PK, Singh P, Yadav D. GLCM based feature extraction and medical X-ray image classification using machine learning techniques. Paper presented at: Proceedings of the IEEE Conference on Information and Communication Technology; 2019:1-6; Allahabad, India. https://doi.org/10.1109/CICT48419. 2019.9066263.

[26] Jogin M, Madhulika MS, Divya GD, Meghana RK, Apoorva S. Feature extraction using convolution neural networks (CNN) and deep learning. Paper presented at: Proceedings of the 2018 3rd IEEE International Conference on Recent Trends in Electronics, Information & Communication Technology (RTEICT); 2018:2319-2323; Bangalore, India: IEEE.

https://doi.org/10.1109/RTEICT42901.2018.9012507.

[27] Chen Y, Jiang H, Li C, Jia X, Ghamisi P. Deep feature extraction and classification of hyperspectral images based on convolutional neural networks. IEEE Trans Geosci Remote Sens Deep. 2016;54:6232-6251.

[28] Alkhayrat M, Aljnidi M, Aljoumaa KA. Comparative dimensionality reduction study in telecom customer segmentation using deep learning and PCA. J Big Data. 2020;7:9. https://doi.org/10.1186/s40537-020-0286-0.

[29] M. Jain, T. AlSkaif, S. Dev, A clustering framework for residential electric demand profiles, in: Proc. International Conference on Smart Energy Systems and Technologies (SEST), IEEE, 2020, pp. 1–6.

[30] M. Jain, T. AlSkaif, S. Dev, Validating clustering frameworks for electric load demand profiles, IEEE Trans. Ind. Inform. 17 (12) (2021) 8057–8065, http://dx.doi.org/10.1109/TII.2021.3061470.

[31] S. Dev, Y.H. Lee, S. Winkler, Systematic study of color spaces and components for the segmentation of sky/cloud images, in: Proc. IEEE International Conference on Image Processing (ICIP), IEEE, 2014, pp. 5102–5106.

[32] R.S. Kabade, M. Gaikwad, Segmentation of brain tumour and its area calculation in brain mr images using K-mean clustering and fuzzy C-mean algorithm, International Journal of Computer Science & Engineering Technology 4 (05) (2013) 524–531.

[33] E. Abdel-Maksoud, M. Elmogy, R. Al-Awadi, Brain tumor segmentation based on a hybrid clustering technique, Egypt. Inf. J. 16 (1) (2015) 71–81.

[34] H. Wang, Y. Li, S. Xi, S. Wang, M.S. Pathan, S. Dev, AMDCNet: An attentional multi-directional convolutional network for stereo matching, Displays (2022) 102243.

[35] A. Chaurasia, E. Culurciello, Linknet: Exploiting encoder representations for efficient semantic segmentation, in: 2017 IEEE Visual Communications and Image Processing (VCIP), IEEE, 2017, pp. 1–4.

[36] G.J. Brostow, J. Fauqueur, R. Cipolla, Semantic object classes in video: A high-definition ground truth database, Pattern Recognit. Lett. xx (x) (2008) xx.

[37] Bikas S, Reyes M, Jakab A, et al. Identifying the best machine learning algorithms for brain tumor segmentation, progression assessment, and overall survival prediction in the BraTS challenge; 2018. arXiv:1811.02629.

[38] Glas AS, Lijmer JG, Prins MH, Bonsel GJ, Bossuyt PMM. The diagnostic odds ratio: a single indicator of test performance. J Clin Epidemiol. 2003;56:1129-1135.

[39] Saxena S, Kumari N, Pattnaik S. Brain tumor segmentation in FLAIR MRI using sliding window texture feature extraction followed by fuzzy C-means clustering. Int J Healthcare Inf Syst Inform. 2021;16(3):1-20. https://doi.org/10.4018/ijhisi.20210701

[40] Saxena S, Mohapatra P, Pattnaik S. Brain tumor and its segmentation from brain MRI sequences. Early Detection of Neurological Disorders Using Machine Learning Systems, Advances in Medical Technologies and Clinical Practice. Hershey, PA: IGI Global; 2019:39-60. https://doi.org/10.4018/978-1-5225-8567- 1.ch004